

A FINITE ELEMENT MODEL FOR DETERMINING THE EFFECT OF PERIPHERAL BLOOD FLOW ON THE FINGER TEMPERATURE

Ying HE¹, Minoru SHIRAZAKI², and Ryutaro HIMENO³

¹Computer and Information Division, RIKEN
2-1 Hirosawa, Wako-shi, Saitama 351-0198, Japan
e-mail: heyings@postman.riken.go.jp

²Computer and Information Division, RIKEN
2-1 Hirosawa, Wako-shi, Saitama 351-0198, Japan
e-mail: shirazak@postman.riken.go.jp

³Computer and Information Division, RIKEN
2-1 Hirosawa, Wako-shi, Saitama 351-0198, Japan
e-mail: himeno@postman.riken.go.jp

Abstract

A two-dimensional thermo-fluid FE model is presented to investigate the effect of blood flow on the temperature distribution of a finger. The modeled finger consists of the countercurrent larger artery and vein, bone, tendon and skin. The basic Navier-Stokes equations and energy equation are used to express the flow inside the blood vessels. The thermal transport inside the solid tissues is expressed by the Pennes bioheat equation, and the Galerkin finite element technique is used in the discretization of the governing equations. The blood pressure and velocity are solved by a fractional step method, and the temperature within the blood vessels and tissues is solved explicitly. The temperature distributions at different blood velocities were obtained, and the computed temperatures are compared with the measured values. The simulated results show that the variation in finger skin temperature was much less than that of the blood velocity.

Nomenclature

$Bi=hD/\lambda$	Biot number, indicating the dimensionless ratio between heat convected to the environment and heat conducted inside the tissue
c	specific heat, J/kgK
D	diameter of blood vessel, m
E_{sk}^*	evaporative heat loss, W/m ²
E_{sk}	dimensionless evaporative heat
h_c	convective heat transfer coefficient, W/m ² K
h_{ra}	radiative heat transfer coefficient, W/m ² K
h_e	evaporative coefficient, W/m ² kPa
P_s^*	water vapor pressure at the skin surface, kPa
$P=P^*/\rho U_\infty^2$	dimensionless pressure
P_{amb}^*	water vapor pressure in the environment, kPa
q_{met}^*	metabolic heat generation, W/m ³
q_{met}	dimensionless metabolic heat generation
$Pe=U_\infty D/\alpha$	Peclet number
$Re=U_\infty D/\nu$	Reynolds number

t^*	time, s
$t=t^*/D/U_\infty$	dimensionless time
u and v	dimensionless velocity in the x and y directions
W	dimensionless volumetric blood perfusion rate
x and y	dimensionless coordinates
α	thermal diffusivity, m^2/s
Γ	boundary surface
λ	thermal conductivity, W/mK
μ	viscosity, kg/s.m
ν	kinematic viscosity, m^2/s
ρ	mass density, kg/m^3
ω	blood perfusion rate, 1/s
ψ	dimensionless ratio of blood to tissue thermal inertia

Subscripts

a	artery
amb	ambient
b	blood
s	skin
t	tissue
∞	characteristic parameter
m	mean

Superscripts

n, n+1	index of the time step
--------	------------------------

Introduction

Temperature influences all forms of life and all substances. For the past few decades, the relationship between man and his thermal environment has always been attractive to researchers. The human finger has a high sensory capability that can convey information about mechanical, thermal and tissue damaging events. Investigating the thermal characteristics of the human finger is an important topic because it is essential for understanding the vaso-constrictive and hyperemic response of peripheral blood vessels.

It is known that the finger skin temperature is closely related to the total digital blood flow. For example, after cigarette smoking, the peripheral circulation becomes worse and the skin temperature decreases. When a person is in a state of stress, the finger skin temperature will decrease for vasoconstriction of the finger arterioles. On the other hand, while warming distant body torso areas, the blood circulation to the fingers will be augmented and the fingers will be at a comfortable temperature during cold exposure.

Several models concerned with the thermal behavior of one part of the human body have been developed. Yokoyama *et al.* (16) have proposed a computer model to investigate the cold-stressed effects in the finger. They created a physiological model of the finger based on measured data and the anatomical structure. The finger consists of bone, tendon and skin, and the heat transfer process is depicted by three equations related to the tissue, and arterial and venous pool.

Ling *et al.* (10) have proposed an FE model to investigate the cooling effects of water bags on a human leg, the modeled leg consisting of skin, fat, bones and two main arteries. The

Pennes bio-heat equation was applied. The blood perfusion term was assumed to be a function of the local tissue temperature, and they considered the blood flow inside the main arteries as non-Newtonian laminar flow.

Sihtzer *et al.* (14) have presented a thermal model to represent an extremity such as a finger. This model incorporates not only the effects of heat conduction, metabolic heat generation, and thermal transport by blood perfusion, but also heat exchange between the tissue and the larger blood vessels, and arterio-venous heat exchange. The heat transfer coefficient for the major blood vessels is defined by a relationship involving the blood vessel radius, ‘influence volume’ radius, cylinder radius, and thermal conductivity.

All these models have their particular characteristics, including the effects of blood vessels. However, some aspects need further investigation, particularly the effect of blood flow rate on the finger temperature.

We present in this work a thermo-fluid FE model to investigate the effect of blood flow on a finger. We include the influence of large blood vessels embedded in the perfused tissue, the blood flow inside these large blood vessels being assumed to be developed laminar flow that can be described by the Navier-Stokes equations. The thermal transport in the blood vessels is expressed by the energy equation, and the thermal transport in the tissue is described by the Pennes bioheat equation. Discretization of these equations was done by using the Galerkin finite element technique. The velocity and temperature profiles in the blood vessels and temperature distribution in the tissues are simultaneously obtained. It is expected that this thermo-fluid FE model will be applicable to health management for monitoring physiological parameters and to the robot industry.

Finger model and governing equations

Fig. 1 shows a schematic diagram of the modeled finger section in the longitudinal direction. The arterial blood enters *via* the large blood vessels in the two sides of the finger, and exits as venous blood. The model for this blood vessel structure was developed from the countercurrent heat exchange model of Mitchel and Myers (5). Bone and tendon surround the large blood vessels, and the external tissue is skin. We have not considered the connection of capillaries between the arteries and veins, and we believe that the influence on heat transfer of the blood flow in these capillaries can be neglected.

Laminar flow convection is assumed in the large blood vessels. We are currently neglecting the tube elasticity by assuming that the blood vessels are rigid, and the blood is assumed to be an incompressible Newtonian fluid. In order to solve the blood flow and solid tissue parts simultaneously, we have assumed the solid tissue to be a fluid with zero flow velocity.

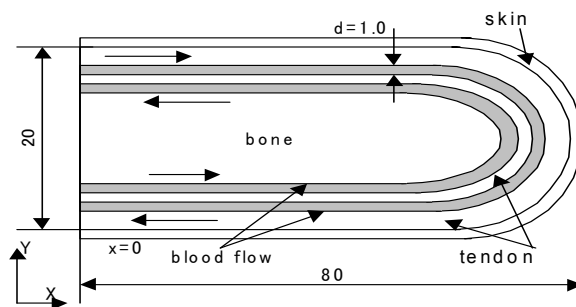


Fig. 1 Schematic diagram of the finger section in the longitudinal direction

The mass and momentum equations in the whole area can be expressed as follows:

$$\frac{\partial u}{\partial x} + \frac{\partial v}{\partial y} = 0 \quad (1)$$

$$\frac{\partial u}{\partial t} + u \frac{\partial u}{\partial x} + v \frac{\partial u}{\partial y} = -\frac{\partial P}{\partial x} + \frac{1}{\text{Re}} \left(\frac{\partial^2 u}{\partial x^2} + \frac{\partial^2 u}{\partial y^2} \right) \quad (2)$$

$$\frac{\partial v}{\partial t} + u \frac{\partial v}{\partial x} + v \frac{\partial v}{\partial y} = -\frac{\partial P}{\partial y} + \frac{1}{\text{Re}} \left(\frac{\partial^2 v}{\partial x^2} + \frac{\partial^2 v}{\partial y^2} \right) \quad (3)$$

The energy equation in the blood vessels can be written as:

$$\frac{\partial T}{\partial t} + u \frac{\partial T}{\partial x} + v \frac{\partial T}{\partial y} = \frac{1}{\text{Pe}_b} \left(\frac{\partial^2 T}{\partial x^2} + \frac{\partial^2 T}{\partial y^2} \right) \quad (4)$$

The Pennes bioheat equation is applied to the solid area as follows:

$$\rho c \frac{\partial T^*}{\partial t} = \lambda \left(\frac{\partial^2 T^*}{\partial x^2} + \frac{\partial^2 T^*}{\partial y^2} \right) + \omega_b \rho_b c_b (T_a^* - T^*) + q_{met}^* \quad (5)$$

In order to simultaneously solve the temperature in the blood vessels and solid tissues, we have rewritten the Pennes equation in the following dimensionless form:

$$\frac{\partial T}{\partial t} = \frac{1}{\text{Pe}_t} \left(\frac{\partial^2 T}{\partial x^2} + \frac{\partial^2 T}{\partial y^2} \right) + \frac{\psi}{\text{Pe}_b} W(1-T) + \frac{\psi}{\text{Pe}_b} q_{met} \quad (6)$$

$$\text{where } T = \frac{T^* - T_\infty^*}{T_a^* - T_\infty^*}, \quad \text{Pe}_t = \frac{U_\infty D}{\alpha_t}, \quad \psi = \frac{\rho_b c_b}{\rho c}, \quad W = \frac{(\omega_b \rho_b c_b) D^2}{\lambda_b}, \quad q_{met} = \frac{q_{met}^* D^2}{(T_a^* - T_\infty^*) \lambda_b} \quad (7)$$

Note that α_t refers to the thermal diffusivity of the blood and solid tissues. The energy equation describes the temperature distribution in both the blood flow domain and solid tissue domain. The energy equation becomes the conventional Pennes bioheat equation when the blood flow velocity is zero.

The following boundary conditions are specified:

1. Inlet of arterial blood to the finger

$$u = 1, \quad v = 0, \quad T = 1 \quad (8)$$

2. Outlet of blood from the finger

$$P = P_{out} \quad (9)$$

3. Inside of solid tissue in the finger

$$u = v = 0 \quad (10)$$

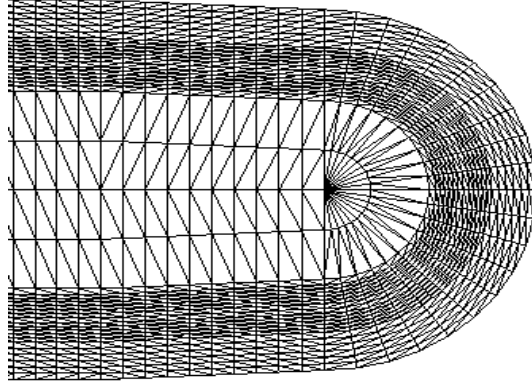


Fig. 2 Finite element grid network of the finger model in the longitudinal direction

4. Solid part at base of the finger

$$u = v = 0, \quad T = f(y) \quad (11)$$

5. Skin surface (in the air)

$$-\lambda_s \frac{\partial T}{\partial n} \Big|_{\Gamma} = h_c (T^* - T_{\infty}^*) \Big|_{\Gamma} + h_{ra} (T^* - T_{\infty}^*) \Big|_{\Gamma} + E_{sk} \quad (12)$$

The dimensionless equation can be rewritten as

$$-\frac{\partial T}{\partial n} \Big|_{\Gamma} = BiT \Big|_{\Gamma} + \frac{h_{ra} D}{\lambda_s} T \Big|_{\Gamma} + E_{sk} \quad (13)$$

where parameter E_{sk} is expressed by

$$E_{sk} = \frac{E_{sk} D}{\lambda(T_a^* - T_{\infty}^*)} \quad (14)$$

The rate of heat transfer conducted to the skin surface is equal to the rate of heat transfer to the air from the surface by convection, radiation and evaporation. It should be noted that it is not necessary to consider the boundary conditions between the blood vessels and solid tissues because the solid tissue has been assumed to be a fluid with zero flow velocity.

The pressure and velocity of blood flow are assumed to initially be zero. The blood vessel is assumed to be at a uniform temperature throughout, while the initial temperatures of the bone, tendon and skin are all assumed to be 0.75 and also uniform throughout.

Numerical method

We used the fractional step method to obtain the velocity of blood flow and the temperature distribution in the following way.

1. Calculate the interim velocity of blood flow from the following equations:

Table 1. Physical properties and blood perfusion rate of individual tissues

	Bone	Tendon	Skin	Blood
ρ (kg/m ³)	1418	1270	1200	993
c (J/kgK)	2094	3768	3391	3300
λ (W/mK)	2.21	0.35	0.37	0.50
ω (ml/ml/min)	2.0/100	3.43/100	24/100	–
$\mu \times 10^6$ (N.s/m ²)	–	–	–	2500
q_{met} (W/m ³)	352	368	273	–

$$\tilde{u} = u^n - \Delta t \left[u^n \frac{\partial u^n}{\partial x} + v^n \frac{\partial u^n}{\partial y} - \frac{1}{\text{Re}} \left(\frac{\partial^2 u}{\partial x^2} + \frac{\partial^2 u}{\partial y^2} \right) \right] \quad (15)$$

$$\tilde{v} = v^n - \Delta t \left[u^n \frac{\partial v^n}{\partial x} + v^n \frac{\partial v^n}{\partial y} - \frac{1}{\text{Re}} \left(\frac{\partial^2 v}{\partial x^2} + \frac{\partial^2 v}{\partial y^2} \right) \right] \quad (16)$$

2. Solve the Poisson equation by the conjugate gradient (CG) method according to the interim blood flow velocity. The derived equation is expressed as:

$$\frac{\partial^2 P}{\partial x^2} + \frac{\partial^2 P}{\partial y^2} = \frac{1}{\Delta t} \left(\frac{\partial \tilde{u}}{\partial x} + \frac{\partial \tilde{v}}{\partial y} \right) \quad (17)$$

3. Calculate the velocity of blood flow for the new step according to the following equations:

$$u^{n+1} = \tilde{u} - \Delta t \frac{\partial P^{n+1}}{\partial x} \quad (18)$$

$$v^{n+1} = \tilde{v} - \Delta t \frac{\partial P^{n+1}}{\partial y} \quad (19)$$

4. Calculate the explicit temperature of the new step by using the derivative of the forward-difference approximation to time.

The discretization of equations 15-19 and 6 and boundary condition 13 were carried out by using the Galerkin finite element technique with triangular finite elements.

Geometric, physical and physiological parameters

The diameter of the large blood vessel is set to be within 1mm according to the actual anatomical structure, this being used as the characteristic length in our calculation. The length of the finger is set to 80mm, and the dimensions of the bone, tendon and skin are taken from the data of Yokayama (16). The thermal properties of the blood, bone, tendon and skin are listed in Table 1.

When the finger is in moving air whose velocity is in the range of $0 < V < 0.15$ m/s, the heat transfer coefficient at the surface of the finger is $4.0 \text{ W/m}^2\text{K}$. With respect to the radiative heat transfer coefficient, we used the constant value of $4.7 \text{ W/m}^2\text{K}$ as representative for the typical indoor temperature (1).

Evaporative heat loss E_{sk} from the skin depends on the difference between the water vapor pressure at the skin and in that in the ambient environment. It can be written as

$$E_{sk}^* = h_e (P_s^* - P_{amb}^*) \quad (20)$$

The evaporative coefficient can be expressed as a function of the air movement by

$$h_e = 124 \sqrt{V_{amb}^*} \quad W / m^2 kPa \quad (21)$$

Results and discussion

Fig. 2 shows one part of the finite element grid network of the modeled finger. Since it was necessary to simultaneously calculate the blood flow and solid tissue field, many factors needed to be considered in generating the mesh. The mesh used for the bone field is the coarsest, and that for the blood area is the finest as shown in Fig. 2.

We employed two different time intervals in the temperature solution: since the diffusivity of momentum is faster than the thermal diffusivity, the time for the blood flow to reach the steady state is far less than the time to reach a stable temperature distribution. Hence, we used the same time interval to solve the velocity and temperature equations before the blood flow reached the steady state, whereas we used a time interval 100 times longer than this to solve the energy equation after the blood flow had reached the steady state. The output pressure was set to 15-20mm of Hg according to the available reference (2). The distal blood velocity was measured by ultrasound equipment (DVM-4300 bi-directional Doppler) to within 0.025-2m/s. Measurements were taken for two subjects, the range of distal blood velocity being 0.05-0.2m/s. Since there is very little variation in the arterial blood temperature, we assumed that the arterial temperature of the finger remained at 37°C. The indoor ambient temperature was set to 19°C.

The modeled finger was subdivided into 19,234 elements, and three different blood flow velocities of 20, 10 and 6cm/s were considered for calculating the respective temperature distribution. Due to the small diameter of the blood vessel, we used an extremely short time interval in the range of 1×10^{-6} - 2×10^{-5} s to ensure stability of the calculation. The isothermal contours with mean blood flow velocities of 20cm/s and 6cm/s are respectively shown in Fig. 3, together with the velocity distribution in the finger-tip part. It can be seen that the blood temperature inside the arteries remained almost constant for the different mean blood flow velocities, whereas the blood temperature inside the veins obviously varied. On the other hand, the temperature in the solid tissues showed very little variation, as Fig. 4 shows for the temperature profile in a cross section of the finger with different Reynolds numbers. We did not change the diameter of the blood vessel in our calculation, so the mean velocities inside the arteries were 20, 10 and 6cm/s. Although the skin temperature increased with increasing blood flow velocity, the temperature did not increase with increasing blood velocity in the other solid tissues, especially in the bone. The variation in skin temperature with the blood flow velocity was less than expected.

It should be pointed out again that it took longer for the temperature to reach the steady state than for the blood velocity, this being in agreement with the work of Bornmyr and Svensson (3).

We measured the skin temperature of the finger by infrared thermography. Fig. 5 shows the temperature of line A in the thermal image of one subject, the mean velocity of blood flow for this subject being 6cm/s. The calculated temperatures are also plotted in this figure. A comparison between the measured temperatures and those calculated from the present two-dimensional model shows reasonable correlation, although the calculated values are lower than the experimental values. The reason for this discrepancy may be that bifurcation

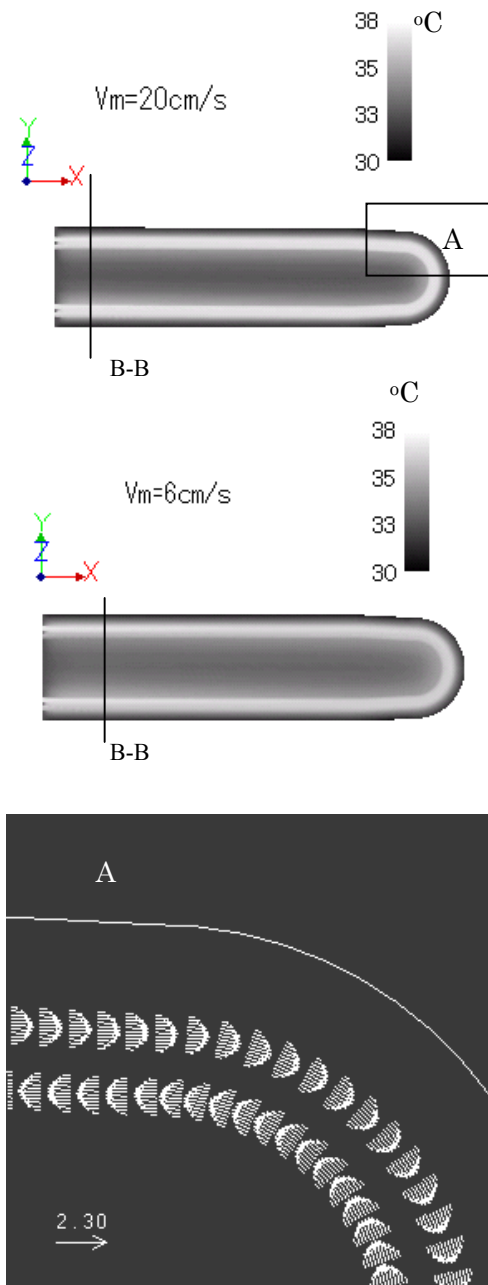


Fig. 3 Isothermal contours and velocity vector of the modeled finger ($T_{\text{amb}} = 19 \text{ }^\circ\text{C}$)

of the arteries and veins has not been considered. Since the heat transported into tissues by bleed-off blood from the arteries and veins has not been included, the computed skin temperatures would be lower.

Concluding remarks

A thermo-fluid FE model has been presented to investigate the effect of blood flow on the temperature distribution of a finger. This model incorporates the effects of blood flow inside the large blood vessels, heat exchange with the large vessels, and blood perfusion. The blood vessels have been assumed to be rigid, and the flow behavior and thermal transport in

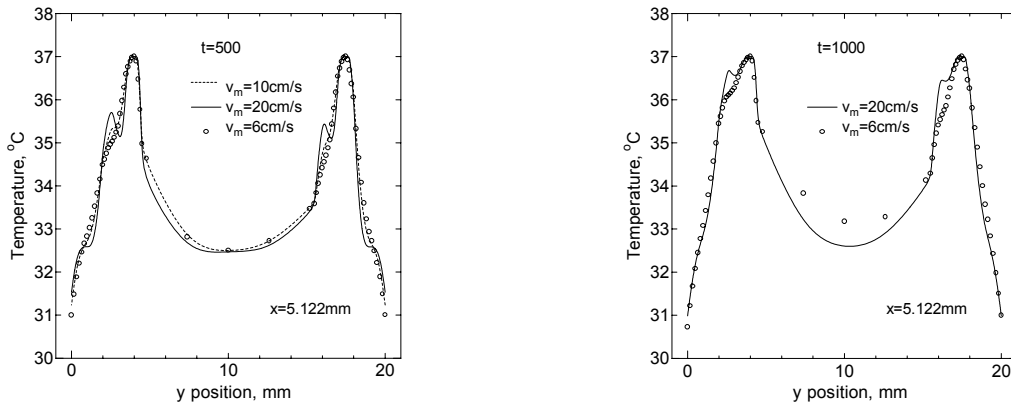


Fig. 4 Temperature profile in a cross section of the finger for different blood flow condition

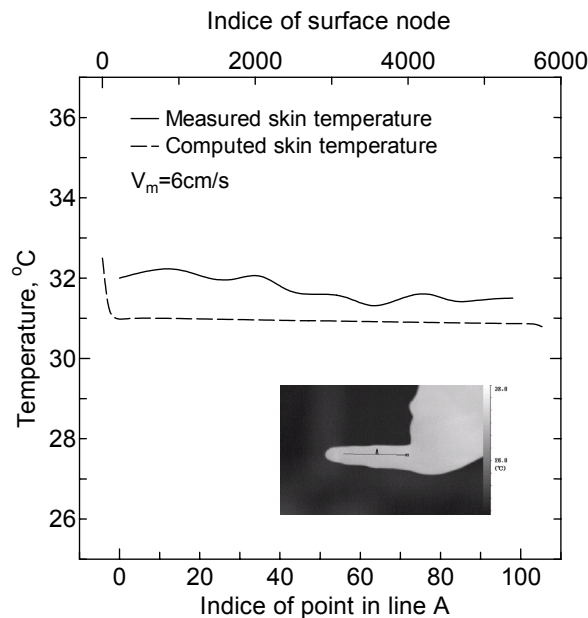


Fig. 5 Comparison of Computed skin temperatures and measured values ($T_{amb}=19^{\circ}\text{C}$)

the vessels and solid tissues have been considered. The main results can be summarized as follows:

1. The temperature distribution in the finger in the longitudinal direction was obtained. There is reasonable correlation between the values for the computed and measured temperature.
2. The skin temperature increased with increasing flow velocity in the large blood vessels in an indoor environment. However, the rise in skin temperature was less than expected for the increase in blood velocity.
3. The lower computed temperatures and the small difference in skin temperature with different blood flow velocities imply that the superficial veins may play an important role in adjusting the skin temperature.

Further research is necessary to investigate the temperature distribution in the finger while receiving internal and external stimuli. In order to investigate the flow and thermal behavior of the peripheral blood circulation, we intend to use a one-dimensional model that includes a

wave-form blood flow, transmural pressure, and temperature.

References

1. 1997 ASHRAE Fundamentals Handbook, ASHRAE Press.
2. Berger, S.A., Physiological fluid mechanics. Introduction to Bioengineering, edited by S. A. Berger, W. Goldsmith, and E. R. Lewis, Oxford University Press, 2000.
3. Bornmyr, S., and Svensson, H., Thermography and laser-Doppler flowmetry for monitoring changes in finger skin blood flow upon cigarette smoking. *Clinical Physiology*, Vol. 11, pp. 135-141 (1991).
4. Clark, R.P., and Edholm, O. G., Man and his thermal environment. Edward Arnold (Publishers) Ltd., 1985.
5. Charny, C.K., Mathematical models of bioheat heat transfer. In Bioengineering Heat Transfer; Advances in Heat Transfer," edited by Y.I. Cho, Vol. 22, pp. 19-155 (1992).
6. Donea, J. Giuliani, S., and Lavel, H., Finite element solution of the unsteady Navier-Stokes equations by a fractional step method. *Computational Methods of Applied Mechanical Engineering*, Vol. 30, pp. 53-73 (1982).
7. He, Y., Kawamura, T., and Himeno, R., A two-dimensional thermal model for determining cold-stressed effects on a human finger. *The 38th National Heat Transfer Symposium of Japan*, pp. 209-210 (2001).
8. Kahle, W., Leonhardt, H., and Platzer, W., Taschenatlas der Anatomie (in Japanese, translated by J. Ochi), pp. 192-246 (1990).
9. Koscheyev, V.S., Leon, G. R., Paul, S., Tanchida, D., and Linder, I. V., Augmentation of blood circulation to the fingers by warming distant body areas. *Eur. J. of Applied Physiology*, Vol. 82, pp. 103-111 (2000).
10. Ling, J. X., Young, I. R., and DeMeester, G., A finite element model for determining the cooling effects of water bags on the temperature distributions of a human leg. *Advances in Heat and Mass Transfer in Biotechnology, ASME, HTD-Vol. 322/BED-Vol. 32*, pp. 69-71 (1995).
11. Pennes, H. H., Analysis of tissue and arterial blood temperatures in the resting human forearm. *J. Applied Physiology*, Vol. 1, No. 2, pp. 93-122 (1948).
12. Rubinsky, B., Heat transfer in biomedical engineering and biotechnology. Proc. of 5th ASME/JSME joint thermal engineering conference, AJTE99-6528 (1999).
13. Sirazaki, M., and Himeno, R., Unified analysis of thermal flows and heat transfer using PC cluster (Japanese). *High Performance Computing Symposium, HPCS2002*, Tsukuba, Japan, pp. 119-124 (2002).
14. Shitzer, A., Stroschein, L.A., Vital, P., Gonzalez, R. R., and Pandolf, K.B., Numerical analysis of an extremity in a cold environment including countercurrent arterio-venous heat exchange. *Trans. ASME, J. Biomechanical Engineering*, Vol. 119, pp. 179-186 (1997).
15. Shitzer, A., Stroschein, L.A., Sharp, M. W., Gonzalez, R. R., and Pandolf, K.B., Simultaneous measurements of finger-tip temperatures and blood perfusion rates in a cold environment. *J. Thermal Biology*, Vol. 22, No. 3, pp. 159-167 (1997).
16. Yokoyama, S., and Ogino, H., Developing computer model for analysis of human cold tolerance. *Annals of Physiological Anthropology*, Vol. 4, No. 2, pp. 183-187 (1985).
17. Xu, X., and Werner, J., A dynamic model of the human-clothing environment system. *Applied Human Science, J. Physiological Anthropology*, Vol. 16, No. 2, pp. 61-75 (1997).